



CONCEPTUAL DESIGN AND PERFORMANCE ANALYSIS OF THE
**EXTENDED Q-RANGE, HIGH PRECISION, HIGH INTENSITY
SMALL ANGLE DIFFRACTOMETER**

FOR SNS

Jinkui Zhao

May 2000

Overview

The 60Hz SNS target offers two important benefits to Small Angle Scattering: broad useable neutron bandwidth and high wavelength resolution. The former makes it possible for simultaneous data collection over a large Q-range. An example is the study of protein-membrane interactions, where protein signals appear at low-Q while lipid signals show up at high-Q (K. He et al, *Biophys. J.* **64**,157,1993). The high wavelength resolution enables resolution of diffraction peaks at high angle. Based on broad scientific interests expressed by the SANS community and recommendations by the SNS Instrument Oversight Committee, we propose an Extended Q-range, High Precision, High Intensity Small Angle Diffractometer at SNS. This document describes the conceptual design and performance analysis of this proposed instrument.

Design Goals

The extended-Q SANS will have the following features:

1. It will have extended Q-range. The smallest accessible Q-value* will be 0.004\AA^{-1} when pinhole geometry is used and 0.001\AA^{-1} when Soller collimators are used. The largest accessible Q-value will be 12\AA^{-1} .
2. It will have high precision. The wavelength resolution, $\Delta\lambda/\lambda$ will be $<1\%$.
3. It will have high intensity. The available flux at sample position with all configurable collimation lengths will be comparable to or better than any existing SANS instruments.

Design Parameters and Choices

The schematic setup of the extended-Q SANS is shown in figure 1. Table 2 summarizes its design and performance parameters.

Machine Length To have the highest useable flux, the instrument has to be as short as possible. The shortest machine length is limited by the angle separation of 13.8° and shielding requirements between two adjacent beamlines. The maximum length for the Extended-Q SANS is chosen at 18m, with sample at 14m^\dagger and a maximum sample to detector distance of 4m. At 14m, the tangential beamline separation will be $\sim 3.36\text{m}$. Taking into account the $\sim 48\text{cm}$ beam bending (through the use of beam bender, see bellow), we will be able to place $\sim 1\text{m}$ shielding materials between neighbors[‡] (we contribute 50cm to each side), and allow a 2m diameter scattering tube be placed at $\sim 1\text{m}$ after the sample. The use of the beam bender requires that the beam upstream from 10m be enclosed tightly by shielding materials. Moveable guides/collimator sections can therefore only be placed between 10 and 14m. Assuming equal source-to-sample

* $Q = (4\pi/\lambda)\sin(\theta)$, where λ is the wavelength of neutrons, 2θ is the scattering angle.

† Unless otherwise noticed, the position parameters in this document are relative to the moderator.

‡ The shielding requirement between beamlines is currently specified at $\sim 2\text{m}$, which is thicker than the number we have taken here. However, the next beamline (in counter clockwise direction) is designed for an Engineering Diffractometer, which will be a long instrument and only curved guides is foreseen at SANS's location. It will therefore provide ~ 1.5 shielding space in tangential direction at 14m from the moderator. The beamline on the other side will likely to be a long instrument as well. Altogether, we should have enough space for shielding.

and sample-to-detector distances for a pinhole SANS, the maximum machine length is then given at 18m.

Moderator The extended-Q SANS will be viewing the top downstream, coupled cold hydrogen moderator on the 60Hz target. At 18 m detector-to-source distance, the maximum useable bandwidth will be $\sim 3.7 \text{ \AA}$. The simulated pulse width of the moderator is $\sim 18 \mu\text{s}/\text{\AA}$, giving a wavelength resolution of $\Delta\lambda/\lambda \sim 0.4\%$.

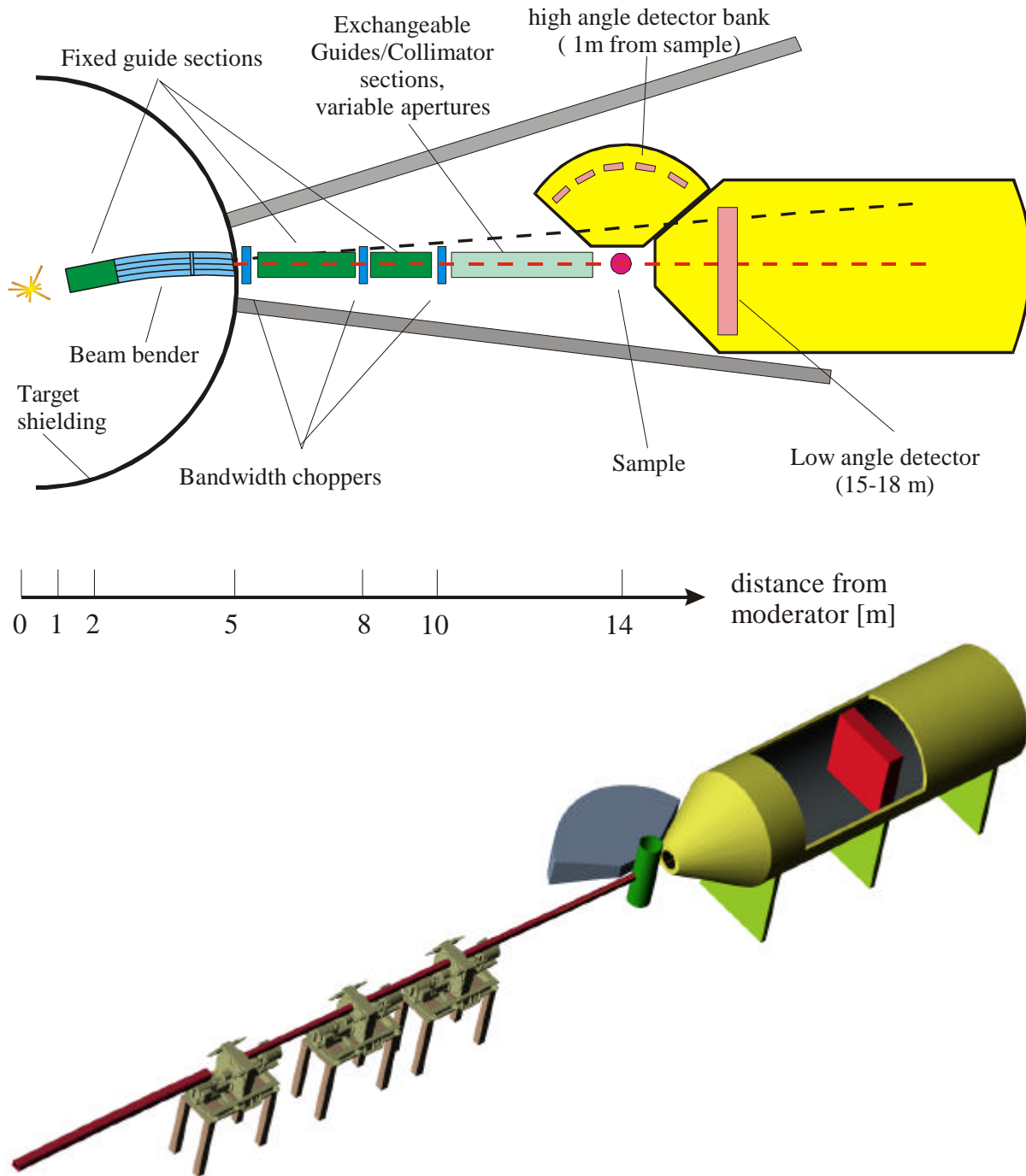


Figure 1. Schematic view (top) and three-dimensional representation (bottom) of the extended-Q SANS.

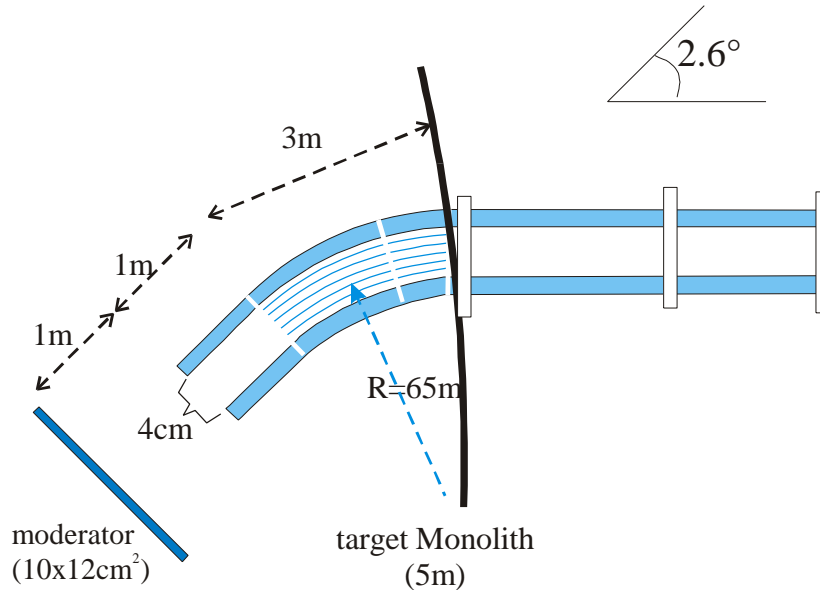


Figure 2 Schematic of the Guide-Bender-Guide system. The three bandwidth choppers at 5, 8, and 10m are indicated.

Beam Bender System A crucial component on the extended-Q SANS is the beam bender system, which is consisted of a straight guide, a beam bender and a further section of straight guide (Figure 2). The purpose of the bender system is to avoid the direct line-of-sight from the moderator. The first 1m-long straight guide is located within the target core vessel insert and starts at 1m from the moderator. The curved, 3m-long multi-channel bender is made of two parts. The first 2m is located within the shutter insert while the remaining 1m extends from the shutter to the edge of the target monolith. The bender has the bending radius of 65m and is divided into 10 bender channels. The straight guide that follows the bender is between 5m and 10m. The cross-section of the guides and bender is $4 \times 4 \text{cm}^2$.

To allow shorter wavelength neutrons to pass through, the bender has to be super-mirror coated. We chose $3.5 \times \text{Ni}$ coating as the baseline design. Better coatings will only enhance the performance. Monte Carlo simulations show that the straight-guide sections will also have to be supermirror coated for maximum performance. Detailed simulations supporting the design choice are attached in appendix B.

Choppers Three standard bandwidth choppers are designed at 5, 8, and 10m. The location of the first chopper is loosely limited between 5 and 5.5m to accommodate possible engineering constraints. The edge of the target monolith is at $\sim 5\text{m}$. This three-chopper system will completely eliminate leakage of slow neutrons (Figure 3).

A T0 chopper is not foreseen. A T0 in place of the beam bender will not be enough to block the fast neutrons. The combination of a T0 chopper with the beam bender will cause some $\sim 15\%$ flux lost. A detailed discussion is attached in appendix B.

Moveable Guide/Collimator sections The last meter before the sample position (13-14m from the moderator) will have no guides. Between 10-13m from the moderator, there will be three

sections of 1m-long, removable guides. The possible collimation lengths will be 1, 2, 3, and 4m. These sections will have to be mounted on vertically sliding rail to enable tight shielding of the direct beam.

In addition, two sections of 2m-long converging Soller collimators will be provided as a user choice. The horizontal collimator will be located between 10-12m and the vertical one will be located between 12-14m. The purpose of these Soller collimators is to converge the direct beam onto a smaller spot on the detector, thus enables the access to smaller Q-values. Two sets of such collimators will be provided, one for high intensity and one for low background (or reflection-free). Both sets are designed for use with 1cm beam stop. For the high intensity set, the entry and exit widths of the collimating channels are 1.67mm and 1.25mm for the horizontal, and

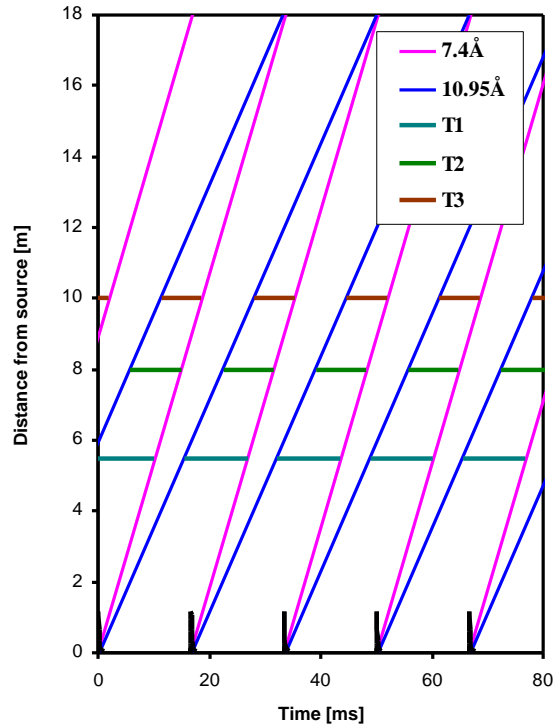
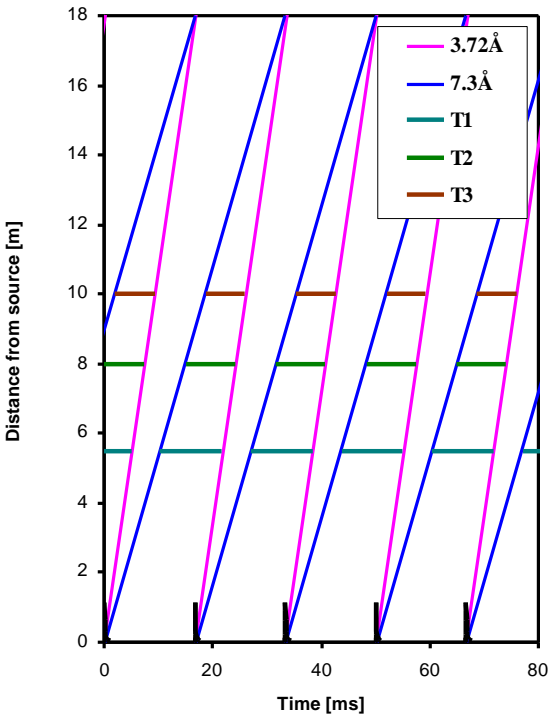
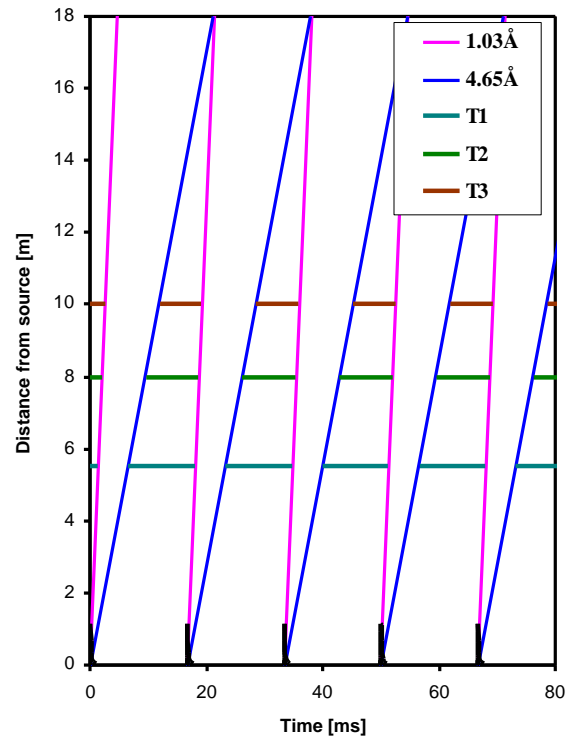


Figure 3. Time diagram of the Extended-Q SANS at the source-to-detector distance of 18-meter. The three figures are for the first (sort of), second, and third-frame operations, respectively. The wavelengths shown are that of the umbra only.

2.5mm and 1.67mm for the vertical collimators, respectively. The low background set will have half these values. Detailed discussion on Soller collimator designs is attached in appendix C.

Detectors The main detector will be a large active area ($1 \times 1 \text{ m}^2$), high counting rate ($\geq 10^6$ neutrons/sec) ^3He detector. The physical resolution of the detector shall be 5 mm. Detector maker ORDELA of Oak Ridge has built a smaller version of such a detector ($64 \times 64 \text{ cm}^2$), which performs well. ORDELA is currently building a $1 \times 1 \text{ m}^2$ detector for the SANS upgrade at HFIR/ORNL. The manufacture specifications on counting rates are $\sim 10^4$ n/s per wire and 10^6 n/s on the whole detector. These detectors have a gas pressure of ~ 1.25 bar and a neutron detection efficiency of $\sim 80\%$ at 5 \AA . The efficiency decreases to $\sim 50\%$ for 2 \AA neutrons. For use on the extended-Q SANS, the detector will have to have about twice the gas pressure to have a reasonable counting efficiency for $1\text{-}5 \text{ \AA}$ neutrons. Increasing gas pressure should be a solvable problem by using convex or concave pressure balancing vessels. Higher gas pressure is also desired since it will improve the spatial resolution, which in turn means more detection wires can be used for increased counting rate.

For experiments on the extended-Q SANS, ORDELA-like detectors will serve most the needs. For experiments with strong scattering samples, detectors with higher counting rate are desirable (see performance section). There are many competing detector technologies currently in development. Some of these efforts are directed at building large area, high counting rate detectors that will be suitable for SANS applications. We will consider these new detecting technologies as they come along.

The detector will be installed in a 5m-long tube to allow variable sample to detector distances between 1- 4 m.

In addition to the main detector, a high-angle detector bank will be installed. It will have five standard, $20 \times 20 \text{ cm}^2$ (active area) detectors, such as those made by ORDELA. The detectors will be arranged on an arc one-meter away from the sample, and cover an angle range of $\sim 35\text{-}150^\circ$.

User access and sample environment At 14 meters from the moderator, there will not be enough space for regular user access from the side. Top access will therefore be provided. There will, however, be about $\sim 1\text{m}$ standing space for checking the sample from the side. Various sample environments, such as automated sample exchanger, furnaces, cryostats, and magnets will have to be lowered in place from the top.

Shielding Shielding after the bender, especially immediately around the beam, will be crucial in reducing the prompt spike. The scattering tube will also have to be shielded against the prompt pulse that is not directly coming from the beam channel. Experiences at ISIS (Henan, private communication) show that painting the scattering tube on the inside with gadolinium oxide and waxing it on the outside with borated wax is an effective method.

Performance estimation

Q-range The minimum accessible Q value on the extended-Q SANS is obtained when the low angle detector is at its maximum distance of 18m (4m detector-to-sample). For circular beam

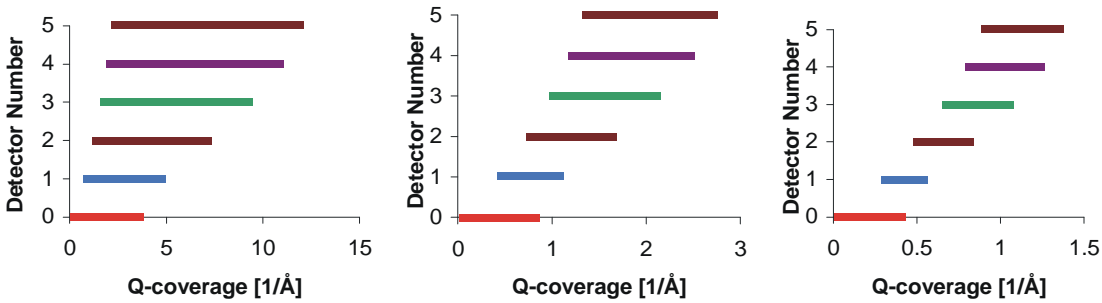


Figure 4. Q-coverage for the extended-Q SANS operating in different frames. Detectors are numbered from 0 to 5 starting from the low angle detector. The position of the low angle detector is at 15m. Left: first frame 1 – 5.4 Å, Middle: second frame 4.4 – 8.8Å, Right: third frame 8.8-13.2Å.

geometry with a 1cm sample and 2cm source apertures (source at 10m), a 4cm beamstop will be needed, giving Q_{min} values of ~ 0.01 , 0.006 , and 0.004\AA^{-1} for instrument operating in the first ($\sim 1-4.7\text{\AA}$), second ($\sim 3.7-7.3\text{\AA}$), and third ($\sim 7.3-11\text{\AA}$) frames, respectively. With the use of Soller collimators, the Q_{min} values for the three frames will be ~ 0.0024 , 0.0015 , and 0.001\AA^{-1} , respectively.

The Q_{max} value on the extended-Q SANS will be 12\AA^{-1} , which is given by the use of 1\AA neutrons at the highest detector angle of $\sim 150^\circ$. Figure 4 shows the Q-coverage of all the detectors.

The largest *continues* Q-coverage of $0.01-12\text{\AA}^{-1}$ is given by operating in the first frame and the low angle detector is at 18m. If Soller collimators are used, the range will be $\sim 0.0024-12\text{\AA}^{-1}$.

The maximum dynamic Q-range on the low angle detector will be >100 . With Soller collimators and includes high angle detectors, a dynamic range of close to 5000 can be reached.

Resolution At low scattering angles, the resolution function ($\Delta Q/Q$) is dominated by geometrical factors. These factors are the sizes and relative positions of the source and sample apertures, and

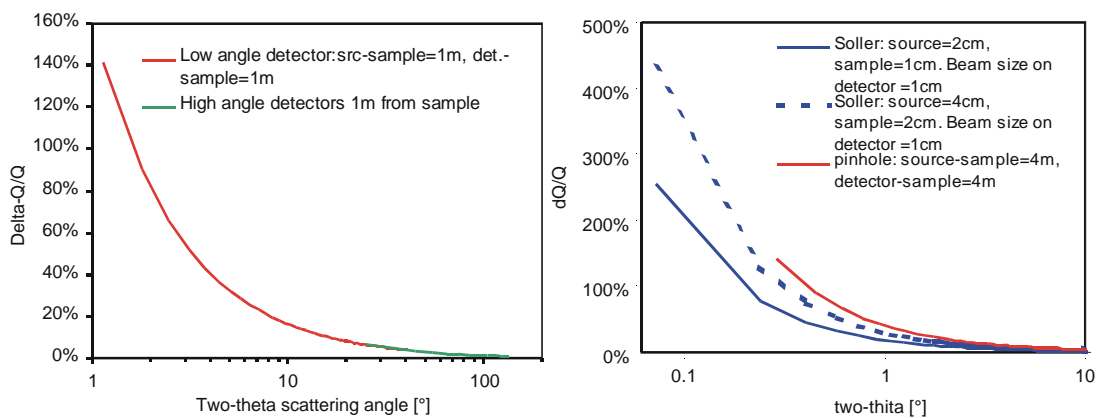


Figure 5. Q-resolution. Left: low-angle detector at 15m. Right: Low angle detector at 18m. Resolutions for Soller collimators with two different sample and source sizes are also shown. Detector pixel resolution of 0.5cm is assumed. The source and sample apertures for pinhole setups are 2 and 1cm, respectively.

pixel resolution of the detector. In back scattering directions, the geometrical contribution reduces to the level of wavelength spread. $\Delta\lambda/\lambda$ is determined by the pulse width of the moderator and detector to moderator distances (figure 5) and is 0.4% on the high angle detectors, 0.4 - 0.5% on the low angle detectors.

The use of Soller collimators will improve the resolution for same detector distance (figure 5). However, the resolution will be worse than pinhole setups with same Q_{min} -values. The Q_{min} -equivalent pinhole setup for the designed Soller collimators is when detector-to-sample distance is 16m. Detailed discussions on resolution and resolution for Soller collimators are attached in appendix D and C.

Flux and Intensity: At the end of the fixed guide systems at 10m, the time-averaged, per Å flux on the extended-Q SANS will be comparable to the new SANS at the HFIR upgrade (Figure 6). The performance of the new HFIR SANS is calculated to be similar the D22 at ILL, which is the best SANS machine currently in operation.

When operating in the second frame and with 4m-collimation length, the flux at sample position integrated over the wavelength band (3.66-7.33 Å for detector at 18m) is 2.5 times that of the planned new HFIR SANS operating at $\Delta\lambda/\lambda=10\%$ (figures 7,8). The gain increases to 7 at 1m-collimation. These ratios reduce to 1.5 and 5 when operating in the third frame (7.33-10.99 Å for detector at 18m).

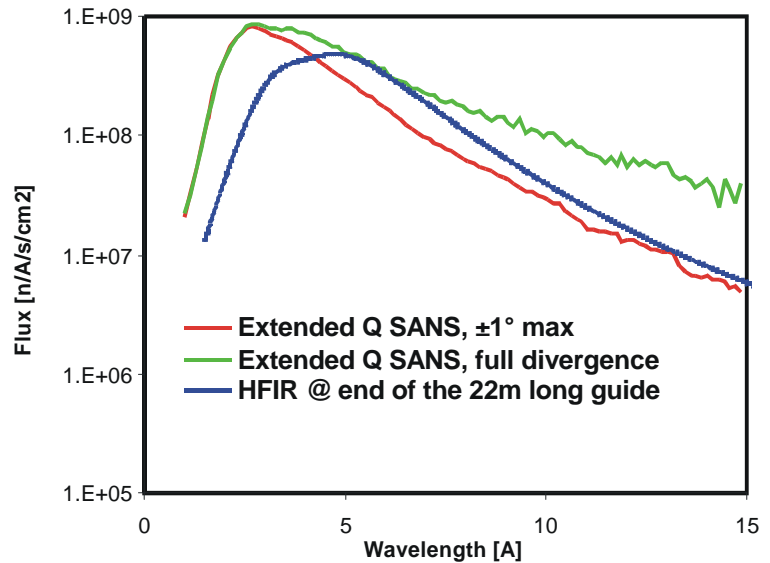


Figure 6. Fluxes at the end of the straight guide at 10m. The downturn below $\sim 2.5\text{\AA}$ is only partially due to the transmission of the beam bender (compare to appendix A, figure A1). Replacing the bender with a T0-chopper will improve the flux in this region (appendix B, figure B5), but will decrease the flux for longer wavelength neutrons (see appendix B) the equivalent location at the planned new SANS at the HFIR upgrade is at the end of a 22m-long straight guide (Ralph Moon/HFIR, private communication).

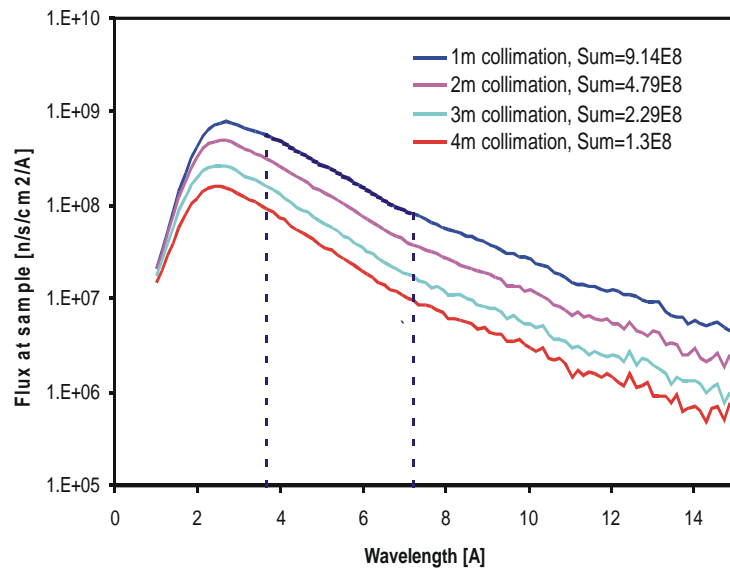


Figure 7. Simulated, time averaged flux at sample position. The region between the dotted lines corresponds to the second frame when detector is at 18m. The 'sums' in the legend are the integrated flux within the second frame.

The detector data rate depends on the sample. Figure 7 shows the simulated available flux at the sample position for different collimation lengths. As a reference, we estimate the maximum per-pixel counting rate in the second frame for an incoherent scatter (such as water), 1cm^2 in cross-section and 50% in transmission. On a $5\text{mm} \times 5\text{mm}$ detector pixel, the maximum instantaneous counting rate will be $\sim 650\text{n/s}$ when the detector is at 15m (1m detector to sample and 1m collimation). At 4m -collimation and with the detector at 18m , the counting rate will be $\sim 60\text{n/s}$.

Data collection time depends both on scattering properties of the sample and on the required Q-range. For strong scatters, such as polymers at high concentrations, collection of a single data set within one minute will be possible for all accessible

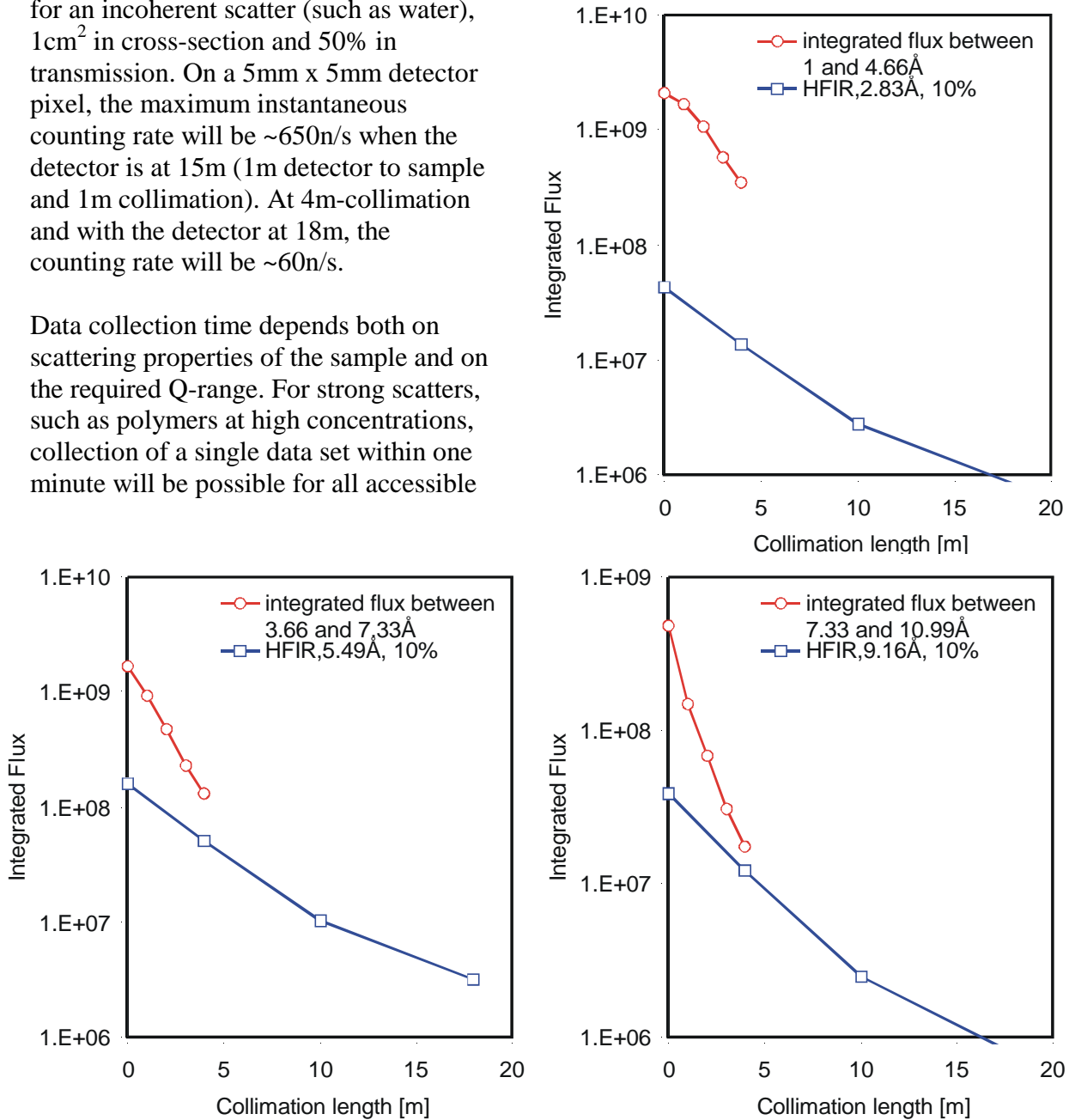


Figure 8 Integrated flux at sample position vs. collimation length in the first (top), second (bottom-left) and third (bottom-right) frames for detector at 18m . Flux integration for planned new SANS at HFIR upgrade (Ralph Moon/HFIR, private communication) is taken in the middle of each frame with 10% $D1 / 1$ FWHM. The flux ratios to HFIR-SANS in the second frame are 2.5 and 7 at 4 and 1m collimations, respectively. In the third frame, these ratios are 1.5 and 5.

Note that the new HFIR SANS is not designed to operate in the wavelength range of the first frame. The first frame figure is therefore for reference only.

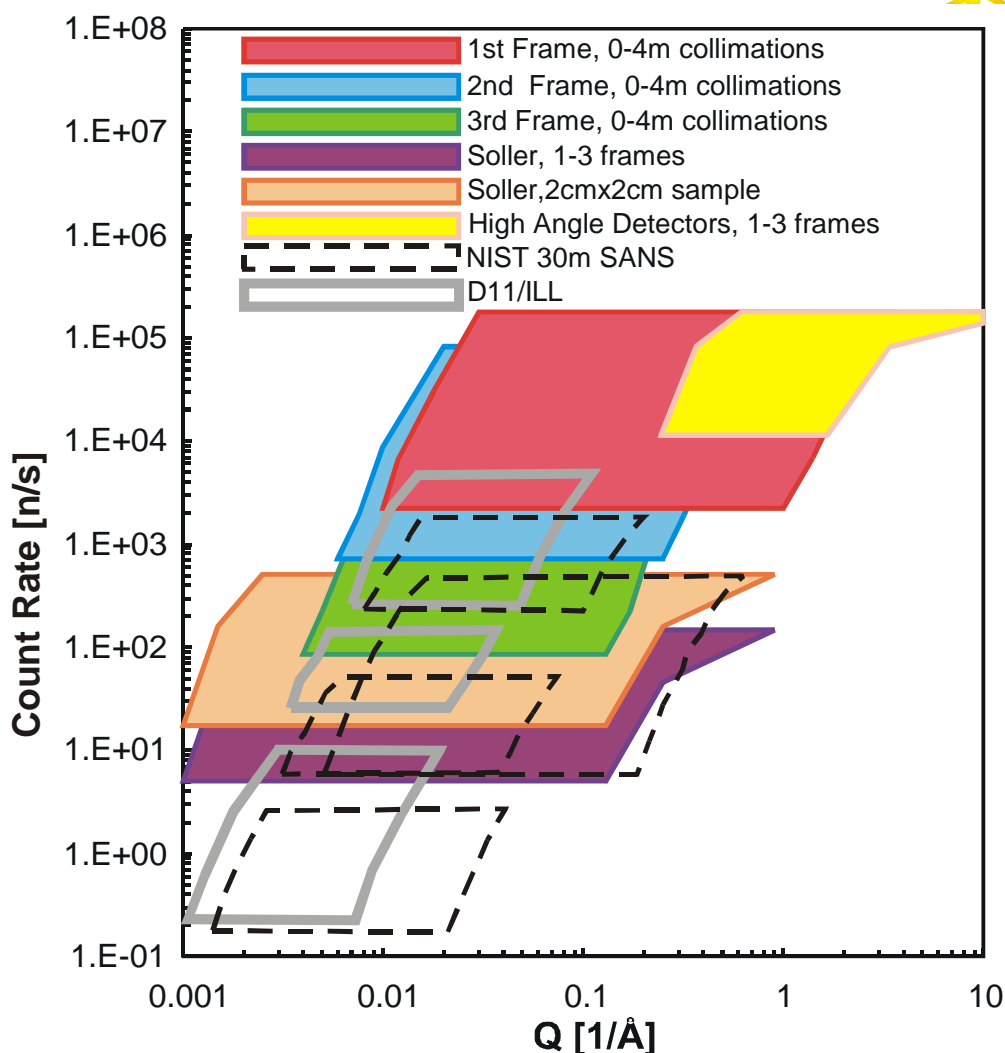


Figure 9 Simulated count rate vs. accessible Q-range. The rate is calculated, as in “Glinka et. al., *J. Appl. Cryst.* 1998, vol 31, 430-445”, by multiplying flux on sample with sample area and the solid angle of a detector pixel. The sample area for all calculations is assumed to be 1cm^2 . The detector pixels for the extend-Q SANS is scaled to $1\text{cm} \times 1\text{cm}$ to match the condition with the NIST SANS. The D11/ILL data was adapted in Glinka et al from Lindner et al, *Physica B*, vol 180-181,967-972.

Q ranges. For weak scatters, such as proteins in dilution solutions, the per data set collection time less than 10 min will be possible when $Q_{\text{min}} \sim 0.001 \text{ \AA}^{-1}$ is needed. For $Q_{\text{min}} \sim 0.006 \text{ \AA}^{-1}$, collection of a single data set with sufficient statistics will be possible within 1 min.

The best currently operating SANS in the US is the two 30m SANS machines at the National Institute of Standard and Technology (NIST). The Q-range on the NIST-SANS is $0.0015\text{--}0.6 \text{ \AA}^{-1}$ (*J Appl. Cryst.* Glinka et al, 1998 **31**,430-445, “*The 30m SANS at NIST*”). Table 2 and Figure 9 compare total fluxes on sample vs. accessible Q-Range for the extended-Q SANS with the NIST SANS.

Summary

The extended-Q SANS on the 60 Hz target will be a unique instrument. Its wide Q coverage and high wavelength resolution are unmatched by any existing SANS instruments. The minimum accessible Q-values will be very competitive, especially when Soller collimators are used. It will have the highest useable flux at sample position, and will be about two orders of magnitude higher than currently available SANS instruments in the U.S.

Table 1. Flux on sample vs. Qmin.

Extend-Q SANS				30-Meter SANS, NIST			
Qmin-Qmax [Å ⁻¹]	Qmax/Qmin	Simulated flux ×10 ⁶ [cm ² /n/s]	Simulation conditions		(δλ / λ =15%, reactor at 20MW)		
			Detector to sample [m]	Frame No	Qmin-Qmax [Å ⁻¹]	Qmax/Qm in	Measured flux ×10 ⁶ [cm ² /n/s]
0.001-0.15	150	0.8 ^(s) , 3 ^(s, 2cm)	4	3			
0.0015-0.3	200	7 ^(s) , 25 ^(s, 2cm)	4	2	0.0015-0.013 ^(10Å)	9	0.032
0.004-0.13	33	14	4	3	0.002-0.019 ^(7.5)	10	0.09
0.006-0.25	42	120	4	2	0.003-0.025	8	0.3
0.008-0.35	44	170	3	2	0.0064-0.04	6	1.3
0.01-0.5	50	360	2	2	0.016-0.1	6	6.3
0.02-0.8	40	820	1	2			

^(s) with Soller collimators.

^(2cm) with 2cm diameter sample. The fluxes in these cases are integrated over the whole sample area.

Table 2. Extended-Q SANS parameters

Moderator:	
Rep rate	60 Hz
Power	2 MW
Location	Top down stream
Type	Coupled LH2, Be reflector
Pulse width	~ 18 μs FWHM per Å
Choppers	All choppers are from standard SNS design
T1	5 m
T2	8 m
T3	10 m
Beam bender	
Location	2-4m, 4-5m
Total Length	3 m
Cross-section	4x4 cm ²
Number of Channels	10
Coating	3.5× Ni-θc super mirror
Total Bending angle	2.6 °

Neutron Guides	3.5× Ni- θ c super mirror coatings	
Location	1-2m, 5-10m (fixed) 10-11m, 11-12m, 12-13m (removable)	
Coating	3.5× Ni- θ c super mirror	
Collimation and apertures	collimation: 1,2,3,4 m variable sample aperture: 1-2cm source aperture: 2-4cm Optional Soller collimators	
Beam Tubes	Evacuated (≤ 0.01 mbar) rectangular tube with inner cadmium or gadolinium coating. The two horizontal tube walls have to be part of the shielding.	
Sample environment	Open area to accommodate ancillary equipments.	
Location	14 m	
Size	≤ 2 cm	
Low-Angel Detector	^3He gas technology.	
Size	1 x 1 m ²	
Pixel resolution	5 mm	
Beam stop	4 x 4 cm ² , 1x1 cm ² with Soller collimators.	
Location	15 – 18 m, continues	
High-Angle Detector Bank	^3He gas technology.	
Location	1m from sample.	
Number of detectors	5	
Detector Size	20 x 20 cm ²	
Pixel resolution	5 mm	
Total Angle coverage	35° - 150°	
Scattering chamber	Evacuated (0.01 mbar), 2m diameter cylinder, with gadolinium oxide painting on the inside and borated wax on the outside. Automated detector rail mounted inside.	
Beam Shielding	Stainless steel after the beam bender.	
Data Acquisition	Standard system with online data reduction.	
Q –range		
Q-min	0.004 Å ⁻¹ with pinhole geometry 0.001 Å ⁻¹ with Soller collimators	
Q-max	12Å ⁻¹	
Resolution	Low-angle detector	High-angle detectors.
$\Delta\lambda/\lambda$ (FWHM)	0.4-0.5%	0.5%
$\Delta Q/Q$ (FWHM)	> 5%	<5% ($\leq 1\%$ for back scattering)
Flux and counting rate		
Maximum per 5x5mm ² pixel count rate	650n/s (with incoherent scatter)	

Appendix A Monte Carlo Simulations

Monte Carlo package developed by the author was used to simulate the extended-Q SANS and its components. Unless otherwise specified, all simulations assume the following conditions:

Source: Simulated source spectrum for the top down stream, coupled cold moderator was used (Iverson/SNS, Figure A1). The maximum source divergence used is 1° (except for figure 6). This value was chosen because it is close to the maximum useable divergence for typical experiments on the Extended-Q SANS. Assuming the use of 1cm sample, 2cm source apertures and a minimum collimation length of 1m, the maximum useable divergence will be $\sim 0.86^\circ$. Notice that this value is not the limit on neutron divergence at the sample position. With neutron guide starts at 1m from the moderator (appendix B), the maximum acceptable divergence for the designed neutron optics, is $\sim 4.5^\circ$. For 1-13 Å neutrons, the divergence values are therefore limited by the guide and mirror coatings to $0.35^\circ/\text{Å}$. Beyond 13 Å, all accepted neutrons by the guide system can be transported.

Guides and Bender: Coating for the bender and guides were assumed to have a critical angle 3.5 times that of natural nickel ($3.5 \times \text{Ni}$, or $0.35^\circ/\text{Å}$) and 80% reflectivity. Trapezoidal function was used for reflectivity: neutron reflectivity is 1 if incident angle $\leq 0.1^\circ/\text{Å}$, linearly decrease to 80% if the angle is between $0.1 - 0.35^\circ/\text{Å}$.

The substrate for the inner bender channels was assumed to be transparent. The implication for simulation is that neutrons with incident angles $< 0.35^\circ/\text{Å}$ but not reflected due to the 80% reflectivity will have a second chance to be reflected by the next channel. Depending on the number of channels the bender has, there will be $\sim 3\text{-}5\%$ flux penalty if opaque substrate is assumed.

Flux vs. Collimation: The simulation for flux vs. collimation assumes a 4cm x 4cm source slit at the end of the guide and a 2cm x 2cm slit at the sample position. This configuration was chosen to match the conditions for HFIR simulations.

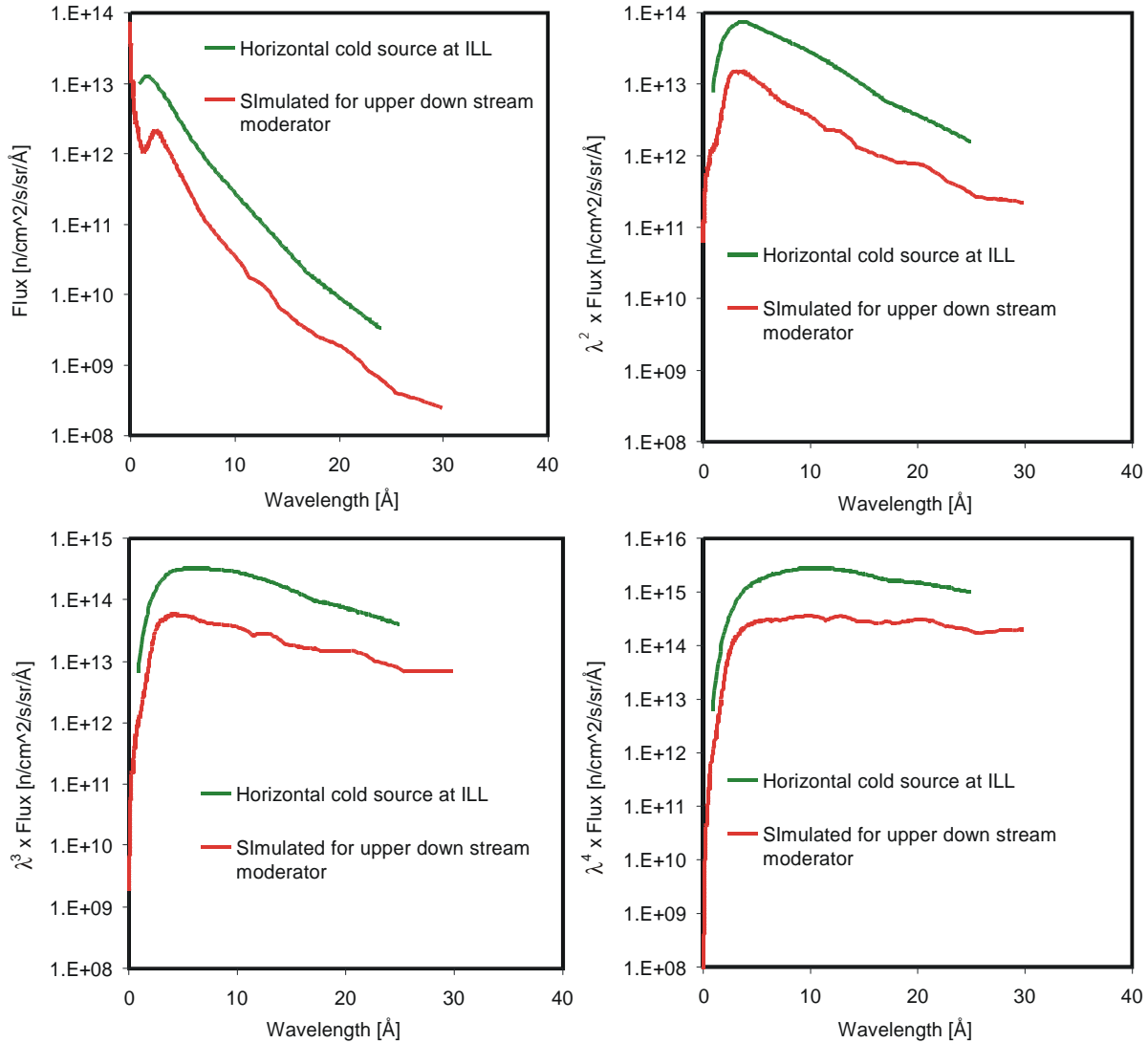


Figure A1 Simulated, time-averaged moderator brilliance for the top-down stream moderator (Iverson/SNS). For comparison, the horizontal cold source at ILL (Ageron, NIM A284,1989,197-199) is shown. Depending on the problem of interest, the scattering power of neutrons can be scaled with wavelength of different orders. Such scaling ranges from λ^2 (Guinier region) to λ^4 (Porod region). Spectra with three different weighting factors are shown. For small angle scattering, the more relevant scaling should be the use of the Guinier region, i.e. λ^2 . In this region, access of same minimal Q-values with shorter λ requires longer collimation length that is inversely proportionally to λ . The flux at sample position is approximately proportional to the inverse of collimation length squared. For other regions and when shorter wavelength is used, data can always be collected at smaller angles to access the same Q-region, without the need of changing collimation length.

Appendix B The Bender System

For the short, 18m SANS instrument, the beam bender should start as early as possible to achieve sufficient beam bending. The closest such place at SNS is ~1m from the moderator within the core vessel insert. At this short distance, radiation and heat damages on the supermirrors could be a concern. Even though experiences at Paul-Scherrer Institute in Switzerland indicate that the supermirrors will most likely be able to endure the strains, we decide to start the beam bender at a safer location of two meters from the moderator, i.e. within the beam shutter.

The chosen bender system is the well-established guide-bender-guide design. The first straight guide section is one meter long and will be located at 1-2m. The curved, multi-channel bender is located between 2-5m, two third of which is inside the main beam shutter (2-4m) and the remaining one third is located between the beam shutter and the edge of the target monolith. A further section of straight guide follows the multi-channel bender (Figure B1).

Bending radius

The bending radius was chosen to be 65m using following criteria: at the position of the last chopper at 10m, where moveable parts of the neutron optics start, there have to be at least 2m of shielding materials blocking the direct view from the moderator. For the 4cm wide neutron beam and assuming 1cm thick guide walls, total blockage of the direct beam will start at ~7m, 2m after the bender (Figure B1). This will give ~3m of shielding space before 10m. The extra 1m over the above-mentioned criteria is to account for the gaps created by the bandwidth choppers at 8m and 10m (Figure 1).

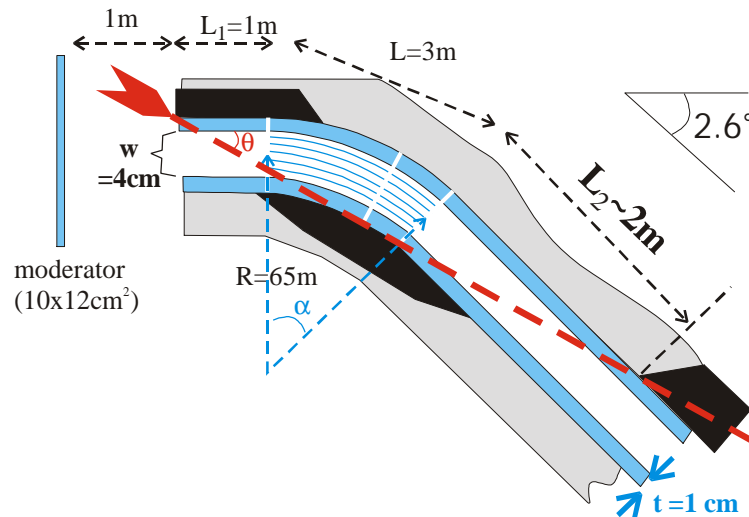


Figure B1 Schematic view of the guide-bender-guide optical system. The system will have to be tightly enclosed by shielding materials (gray shaded area). Locations where shielding is especially important are shaded in black. L_2 is the distance after the bender, at which total blockage of the direct view from the moderator starts. L_2 is determined using the geometrical relations (for the red line):

$$L_2 = xL_1 + R_2 \tan\left(\frac{a}{2}\right)(x-1) \quad \text{with } a = \frac{L}{R}; \quad x = \frac{\sin(q)}{\sin(a-q)};$$

$$q = a \cos\left(\frac{R_1}{\sqrt{R_2^2 + L_1^2}}\right) - a \tan\left(\frac{L_1}{R_2}\right); \quad R_1 = R - \frac{w}{2} - t; \quad \text{and } R_2 = R + \frac{w}{2} + t$$

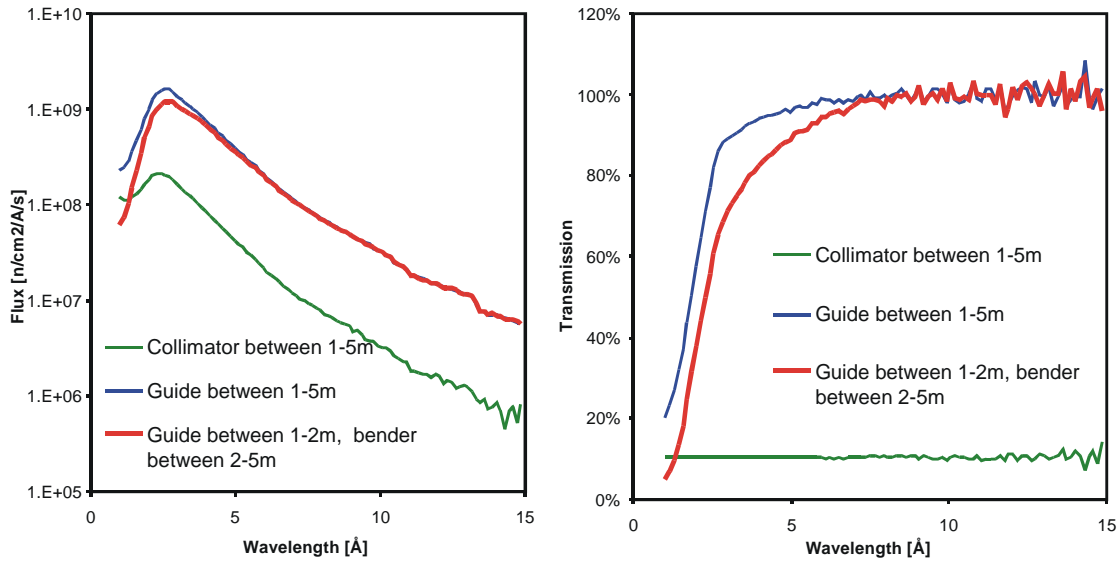


Figure B2. Left: Simulated fluxes at the exit end of the 10-channel, R=65m bender with 1° max source divergence. For comparison, the performances of a straight guide and a collimator are also shown.

Right: Transmissions, as obtained by comparing to the flux at 1m from the moderator.

Number of Bender channels

With the 3.5X-Ni coatings, the number of channels for the bender is optimized to be 10 through Monte-Carlo simulations. The neutron transport property of the bender is shown in figure B2.

For maximum performance, the straight guides before and after the bender will also have to be super-mirror coated. Figure B3 shows the flux comparison at sample position with 3.5X and 1X-Ni coatings. Clearly, there is a big flux lost with 1x-Ni coatings.

To simulate the condition if the straight guide between 1-2m is lost to radiation or heat damages, calculations with this guide section replaced with a collimator were performed (figure B4). The flux is far less critical than if the bender is placed at 1m and damaged.

Alternative bending radii

Engineering constraints on shielding may require more beam bending than the designed bender can provide. We have therefore considered other bending radii as backups. Figure B5 shows the flux ratio at

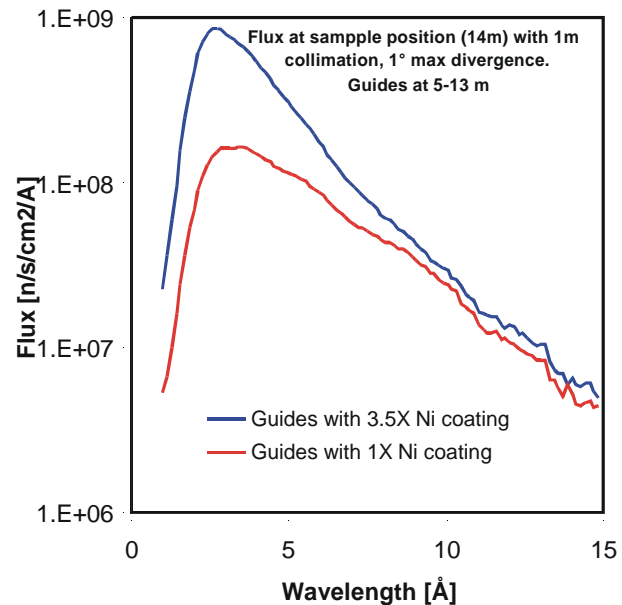


Figure B3 Fluxes at the sample position (14m) with 1m collimation and 1° max source divergence. The coatings for the bender and the guide at 1-2m were kept at 3.5 x Ni. Only coatings for all the guides after bender (8m total) varied.

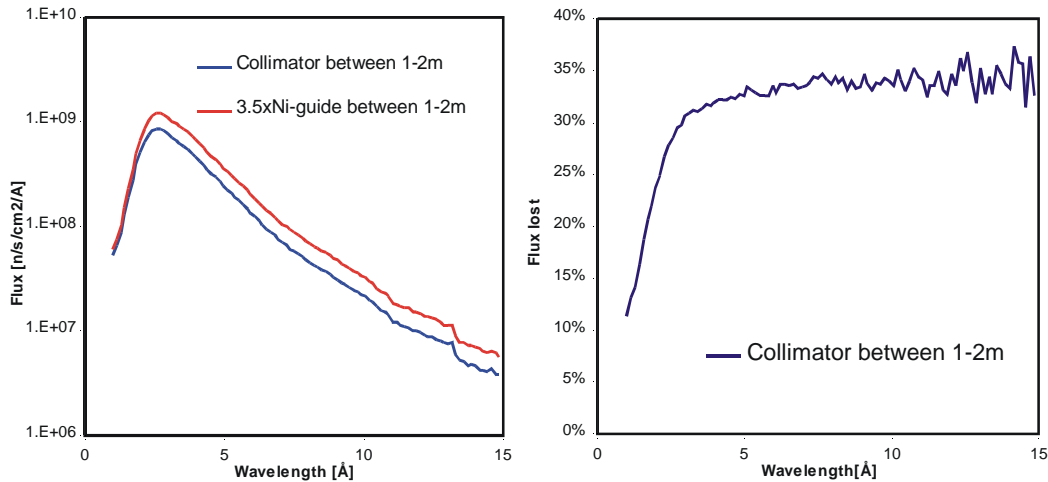


Figure B4. Left: Neutron flux at the end of the bender with 1° max source divergence. Right: Flux lost when the guide between 1-2m is replaced with a collimator.

the end of a 12-channel bender with 50m bending radius as compared with the bender chosen for the extended-Q SANS. The bending radius of 50m would give ~ 4 m total shielding space between the bender and the last chopper at 10m. Even though there is a clear flux penalty at shorter wavelength, such bender could be used as alternative if it is absolutely needed.

T0 chopper as alternative or in addition to the Beam bender

Replacing the bender with a straight guide increases the transmission for short wavelength neutrons (Figure B6). Without the bender, a T0 chopper will then have to be used to block the prompt pulse. The gap associated with the T0 chopper will cause $\sim 15\%$ lost in flux (Figures B6, B7). For experiments that use the second and third frames ($>3.7 \text{ \AA}$), the beam bender will therefore deliver a better performance in term of neutron flux. For operating in the first frame, it is not clear how much the gained flux can translate into gain in signal-to-noise ratio, because the 30cm thick T0 chopper, as is currently designed, will not be enough to block the prompt pulse and thus the background will be worse.

The combination of a beam bender and a T0 chopper does not seem to be necessary, nor does it appear to be a good design choice. The T0 chopper will not be able to have significant contribution to blocking to direct view from the moderator. The flux lost caused by the T0 chopper is also not desired. (Figure B7).

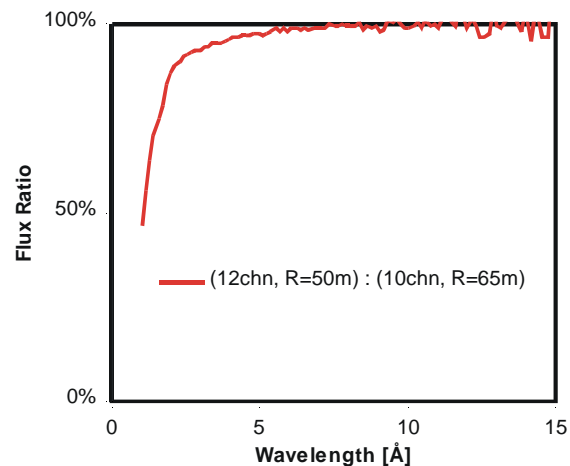


Figure B5. Ratio of simulated fluxes at the end of two benders with different bending radii and channels.

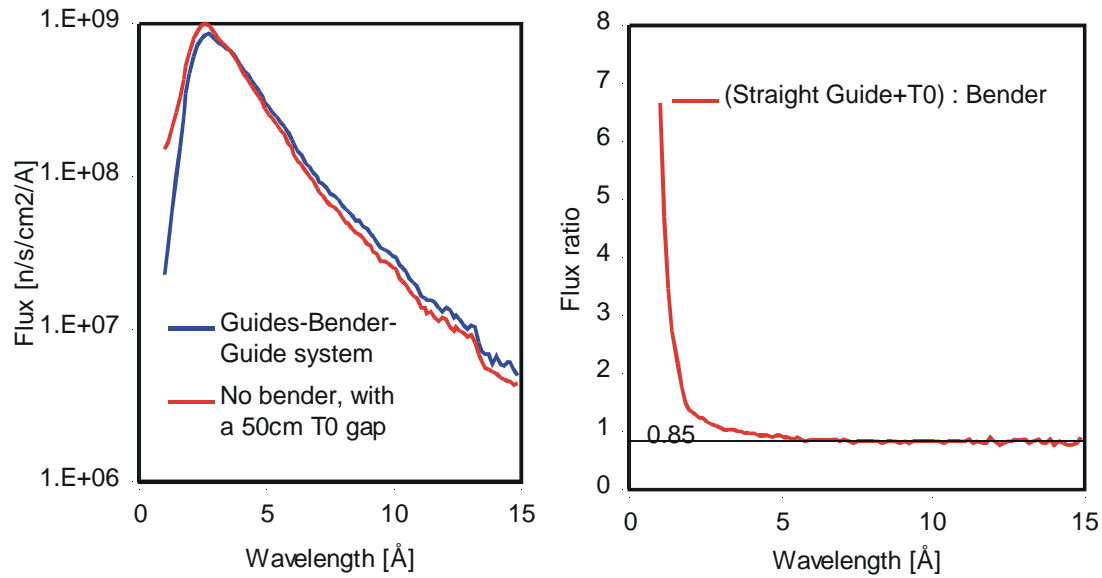


Figure B6 Left: Flux at sample position (14m) with 1m collimation and 1° maximum source divergence. In the case of T0 chopper, the bender is replaced with a straight guide of same coating. A 50cm wide gap is used to emulate the condition of a 30cm T0 chopper. Right: Flux ratio between using T0 chopper and using the bender.

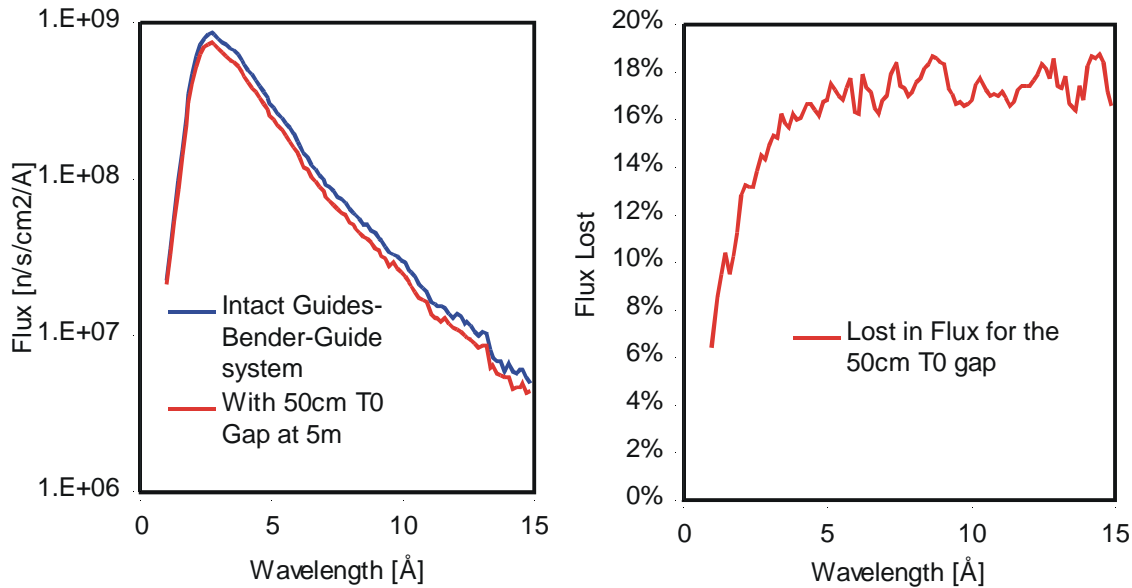


Figure B7 Left: Flux comparison at sample position (14m) with 1m collimation and 1° maximum source divergence. A 50cm wide gap in the guide system is used represent a T0 chopper. Right: Lost in flux caused by the T0 chopper.

Appendix C Soller Collimator

Typical experiments on the extended-Q SANS will have a sample size of ~1cm. For an optimal pinhole setup, we will need a 2cm source aperture and equal sample-to-source and detector-to-sample distances. The direct beam spot size on the detector will then be ~4cm. The minimum accessible Q value is then limited by the size of the beam stop and the maximum sample-to-detector distance. With the maximum machine length of 18m on the extended Q-SANS (4m sample-to-detector), the only way to access smaller Q values is to reduce the size of the direct beam on the detector. Soller collimators provide a nice and simple way to achieve such goal (Crawford/Papagarajan/IPNS).

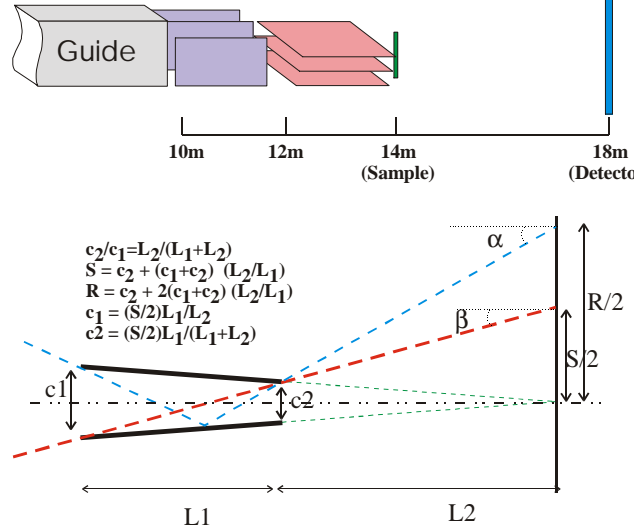


Figure C1. Illustration of the Soller collimators (top) and one collimating channel focusing onto the detector. The beam size on the detector due to first order reflections would be ~ twice that of the direct beam.

Direct Beam size at the detector: The Soller collimator for the extended-Q SANS is designed at 10-12m and 12-14m, each for horizontal and vertical directions, respectively. All collimator channels converge onto the same position on the detector at 18m. The dimensions of a single channel determine the size of the direct beam on the detector (Figures C1, C2). The size of the sample aperture has no effect. In principle, these collimator channels can be made very small. However, because the low-angle detector for the extend-Q SANS has a finite resolution of

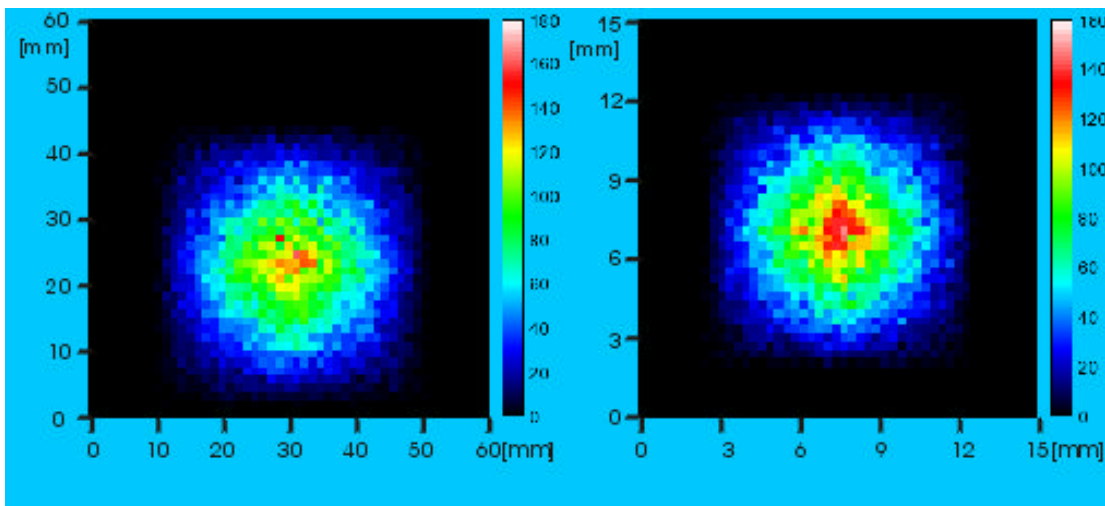


Figure C2. Simulated direct beam on the detector with pinhole setup (left) and Soller collimators (right). For the pinhole setup, sample to source and detector to sample distances are both 16m. The source and sample apertures are 2 and 1cm, respectively. The Soller collimators converge on the detector plane 4m from the sample with designed ‘focusing’ spot of 1cm. Simulations were performed for 10 Å neutrons. The downward shift of the direct beam with respect to the detector center corresponds to the freefall of the neutrons between sample and the detector.

0.5cm, the practical minimal beam size on the detector is limited to ~0.5-1cm. For a 1cm beam spot, the required channel entry and exit widths are 1.67mm and 1.25mm for the horizontal, 2.5mm, and 1.67mm for the vertical collimators, respectively. Half of these values are required for a beam spot size of 0.5 cm.

Minimal accessible Q -value and total flux: For a 1cm beam spot size on the detector, the minimal accessible Q -value on the extended- Q SANS will be equivalent to a pinhole set up with a 16m sample-to-detector distance and a 4cm beam stop. The simulated flux at sample position for both setups is approximately the same (figure C3). Because the sample size has no effect on the accessible Q_{min} , larger samples can be used to increase the total flux in the case of Soller collimator. The practical limit on sample size is $2 \times 2 \text{cm}^2$, which is given by the designed beam cross-section of $4 \times 4 \text{cm}^2$.

Resolution: The tradeoff for the gained Q_{min} and total flux at sample when using Soller collimators is resolution (figure C4). $\delta Q/Q$ with Soller collimators is ~2x that of a 16m pinhole setup with equal sample sizes, and is approximately the same as an 8m pinhole setup (figure C4). Comparing to sample and source apertures, the dimensions of each collimating channel have little contribution to the resolution function. Therefore, to the first order, the direct beam spot size on the detector has no correlation with Q -resolution.

Possible Reflection from collimating channels: Reflections from the collimating channels are possible, even though they should be very weak (ref. IPNS). The spot size on the detector for the first order reflections will be about twice that of the direct beam (figure C1). Therefore, if the collimators are designed to converge onto a 0.5 cm beam spot and a 1cm beamstop is used, the background due to the reflections should be eliminated.

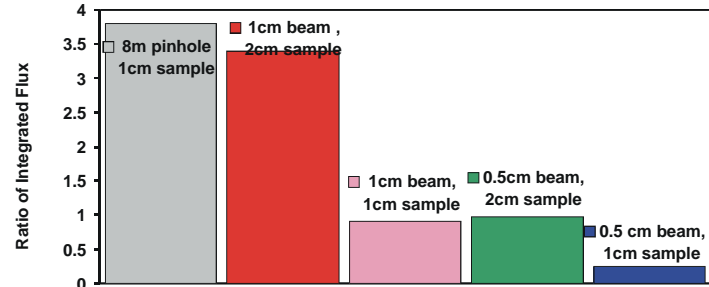


Figure C3 Simulated, integrated fluxes at sample position, shown as ratios to a 16m pinhole geometry (sample-to-detector = detector-to-sample = 16m). The sample apertures for the 16m and 8m pinholes are 1cm. The source apertures for all setups are twice the size of respective sample apertures. The 8m-pinhole has the same resolution as with Soller collimators and 1cm sample aperture (figure C4).

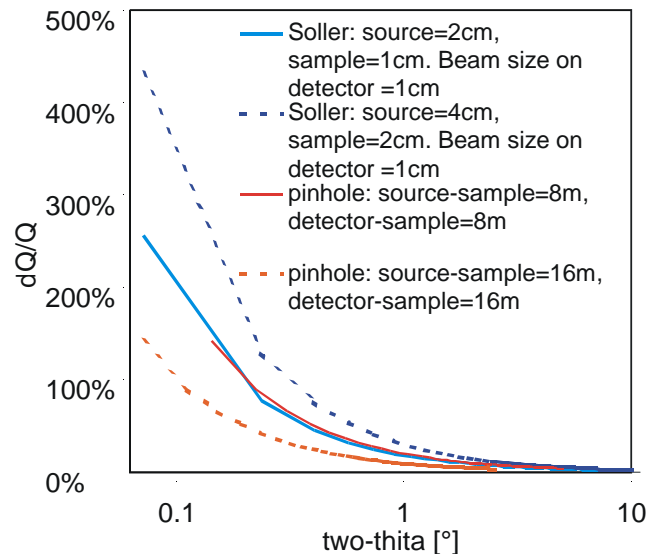


Figure C4 Resolution functions with Soller collimators. Two pinhole setups are also shown. The sample apertures for the pinhole setups are 1cm and the source apertures for all setups are twice their respective sample apertures. The projections of the curves on the two-theta axis correspond to the angular coverage for each setup. The values are calculated using equations derived in appendix D.

Appendix D Resolution Function

Pinhole geometry

The resolution function for momentum transfer $Q = 4\pi/\lambda \sin \mathbf{q}$ has two parts:

$$(\delta Q/Q)^2 = (\delta\lambda/\lambda)^2 + \text{ctan}^2 \mathbf{q} \delta \mathbf{q}^2 \quad (\text{D.1})$$

where λ is neutron wavelength and 2θ is the scattering angle. On a pulsed neutron source, the wavelength resolution is determined by pulse width δt and detector-to-source distance L :

$$(\delta\lambda/\lambda) = \delta t h/m/L = 3.956 \delta t/L \quad (\text{D.2})$$

with δt in [ms/Å] and L in [m]. h is the Planck constant and m is the neutron mass.

For a pinhole set up, the contribution from scattering angle to the resolution in one dimension can be express as (figure D1):

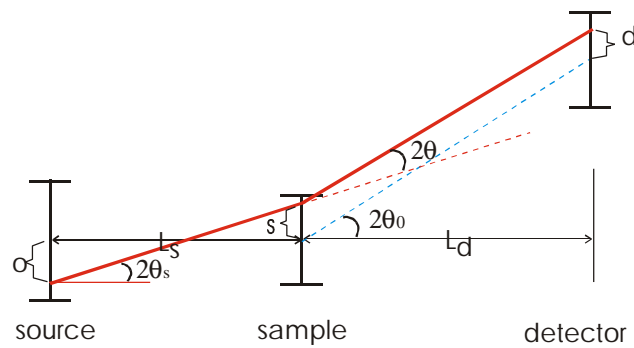
$$\delta \mathbf{q}^2 = 1/4 [\delta o^2/L_s^2 + \delta s^2(1/L_s + 1/L_d)^2 + \delta d^2/L_d^2] \quad (\text{D.3})$$

where o, s , and d represent the source, the sample, and a detector pixel, respectively. L_s is source-to-sample distance. L_d is the sample-to-detector distance. Substituting (D.3) into (D.1), we obtain the full expression for $(\delta Q/Q)$:

$$(\delta Q/Q)^2 = (\delta\lambda/\lambda)^2 + 1/4 \text{ctan}^2 \mathbf{q} [\delta o^2/L_s^2 + \delta s^2(1/L_s + 1/L_d)^2 + \delta d^2/L_d^2] \quad (\text{D.4})$$

For two dimensions, the resolution function is obtained through:

$$\begin{aligned} \delta Q^2 &= \delta Q_x^2 (Q_x/Q)^2 + \delta Q_y^2 (Q_y/Q)^2 \\ &= 1/2 \delta Q_x^2 + 1/2 \delta Q_y^2 \end{aligned}$$



$$2\theta = 2\theta_0 + (d-s)/L_d - (s-o)/L_s$$

$$\delta \theta^2 = 1/4 (\delta o^2/L_s^2 + \delta s^2(1/L_s + 1/L_d)^2 + \delta d^2/L_d^2)$$

Figure D1. Relation of angular resolution to source, sample, and detector pixel sizes in one dimension. The red line represents the pathway of a neutron from position o on source to position s on sample, and detected at position d in a detector pixel.

where we have taken a circular average over the direction of Q . If the source, sample and detector pixel are all square in shape, then equation (D.5) reduces to the form of (D.4).

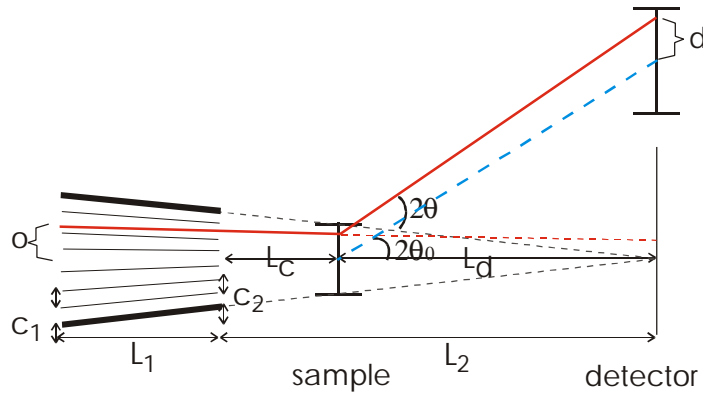
Soller geometry

The angular resolution for a Soller collimator converging onto the center of the detector is (figure D2)

$$\delta q^2 = 1/4 \left[\delta o^2 / (L_1 + L_2)^2 + \delta d^2 / L_d^2 + \delta c_1^2 (L_c / L_1 L_d - 1 / L_1)^2 + \delta c_2^2 (1 / L_d + L_c / L_1 L_d + 1 / L_1)^2 \right] \quad (D.6)$$

c_1 and c_2 are the entry and exit dimensions for one collimating channel, respectively. L_1 is the length of the collimator. L_d is the sample-to-detector distance. L_2 and L_c are the distances from the end of the collimator to detector and sample, respectively.

For Soller collimators with separated x- and y- collimation, the resolution in the x- and y- directions are typically slightly different. Since the samples are typically much larger than the width of a single channel, $\delta\theta$ is dominated by contributions from the size of source and sample.



Visible sample size for one channel:

$$s' = c_2 + (c_1 + c_2) (L_c / L_1)$$

$$\begin{aligned} 2\theta &= 2\theta_0 + (d - s') / L_d - (c_2 - c_1) / L_1 + o / (L_1 + L_2) \\ &= 2\theta_0 + d / L_d - c_2 (1 / L_d + L_c / (L_d L_1) + 1 / L_1) \\ &\quad - c_1 [L_c / (L_d L_1) - 1 / L_1] \\ &\quad + o / (L_1 + L_2) \end{aligned}$$

$$\begin{aligned} 4\delta\theta^2 &= \delta o^2 / (L_1 + L_2)^2 + \delta d^2 / L_d^2 \\ &\quad + \delta c_1^2 (L_c / L_1 L_d - 1 / L_1)^2 + \delta c_2^2 (1 / L_d + L_c / L_1 L_d + 1 / L_1)^2 \end{aligned}$$

Figure D2. Angular resolution for a Soller collimator converging onto the center of the detector. c_1 and c_2 are the entry and exit dimensions for one collimation channel. o, c , and d denotes source, sample and one detector pixel, respectively.